Supporting Information

Strong and Anti-swelling Nanofibrous Hydrogel Composites Inspired by Biological Tissue for Amphibious Motion Sensors

Zheng Ren, [a] Fang Guo [a], Yong Wen [a], Yang Yang [a], Jinxin Liu [a], and Si Cheng*[a]

[a]College of Textile and Clothing Engineering, Soochow University, Suzhou 215123, P. R. China.

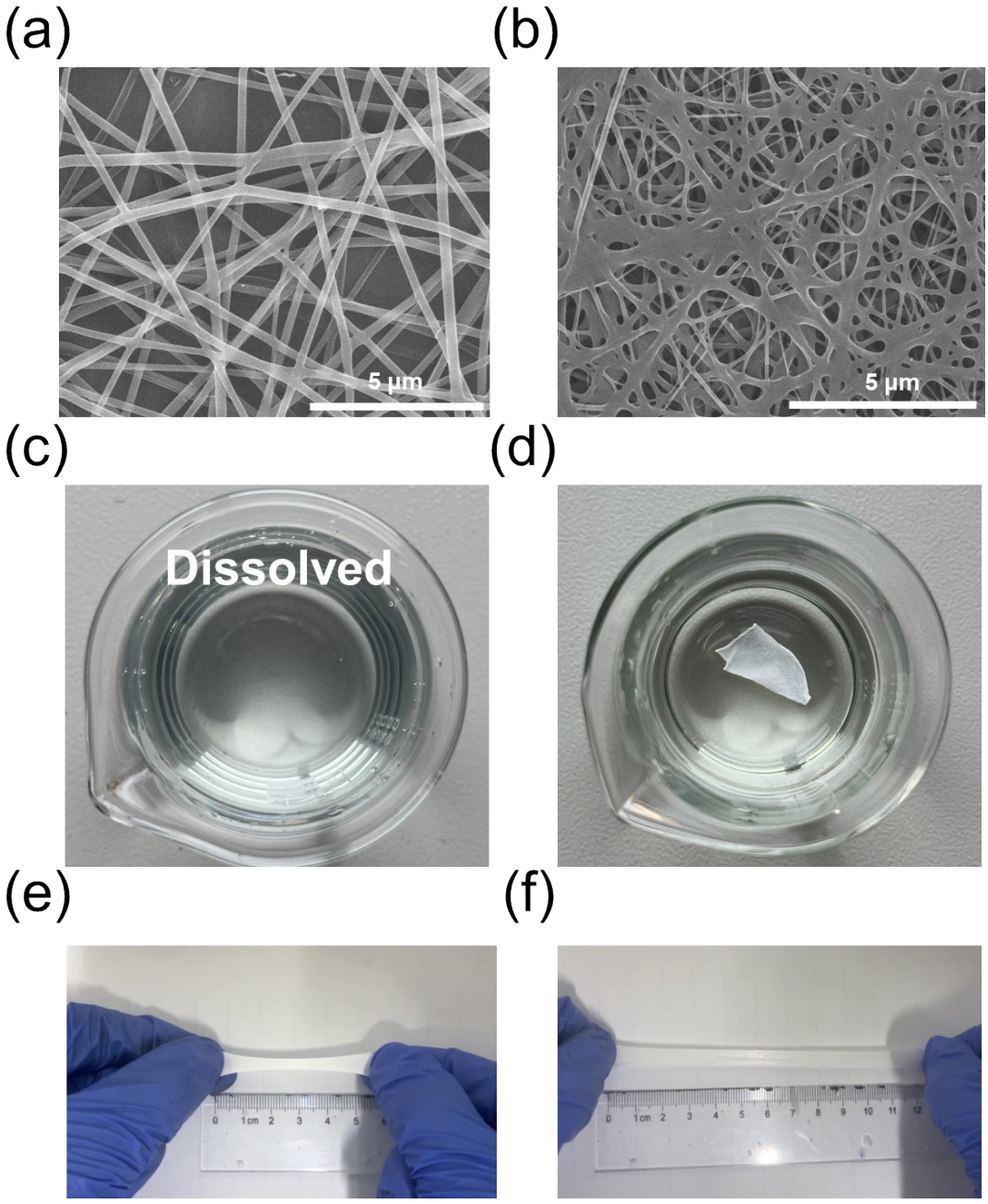

Figure S1. Characterization of PVA and PVAc. (a) SEM images of pure PVA nanofibers membrane. (b) SEM images of PVAc nanofibrous membrane. (c) Digital photograph of the PVA nanofibers membrane shown in Figure S1a when it is immersed in water. (d) Digital photograph of the PVAc nanofibrous membrane shown in Figure S1b when it is immersed in water. (e) Stretchability of the PVA membrane and (f) PVAc nanofibrous hydrogel mat.

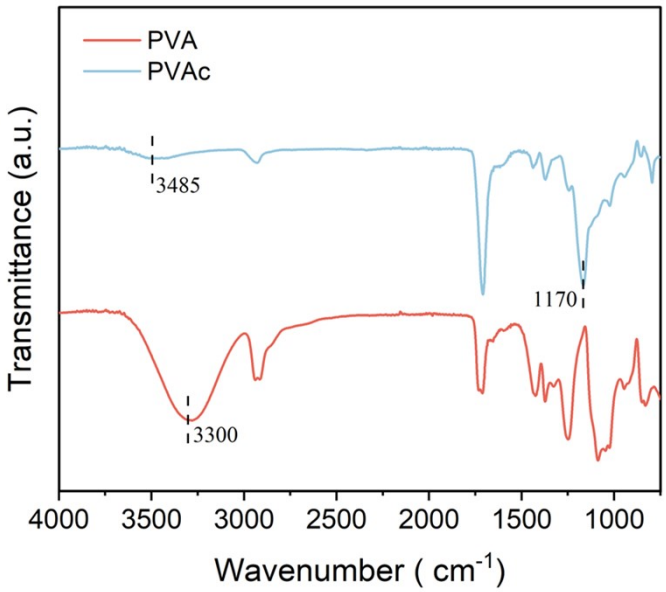

Figure S2. FTIR spectra of PVA and PVAc.

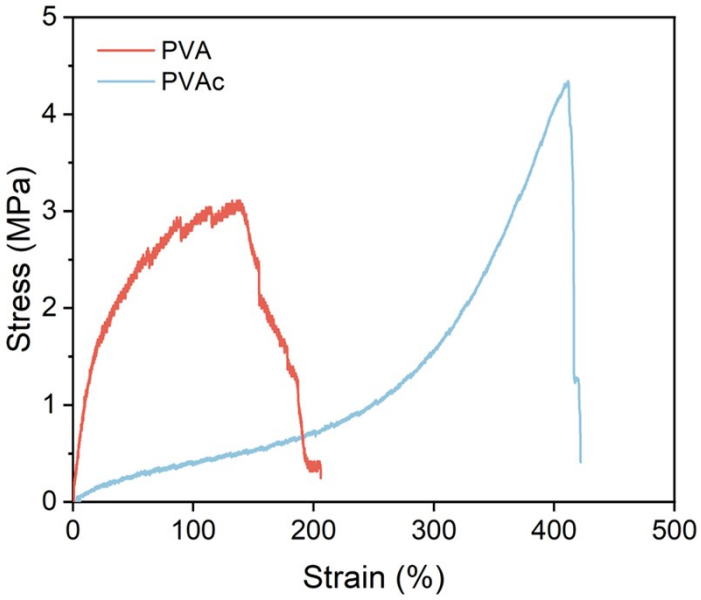

Figure S3. Stress-strain curve of PVA and PVAc.

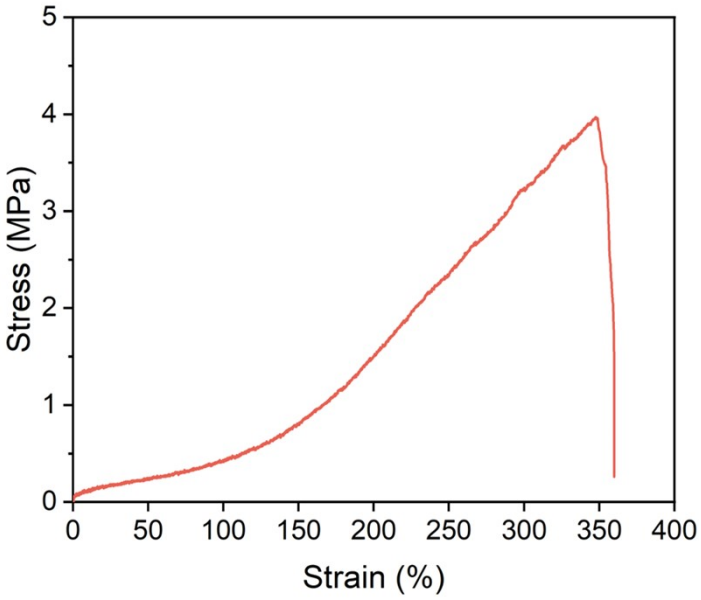

Figure S4. Stress-strain curve of PVAc after immersing in water for 30 days.

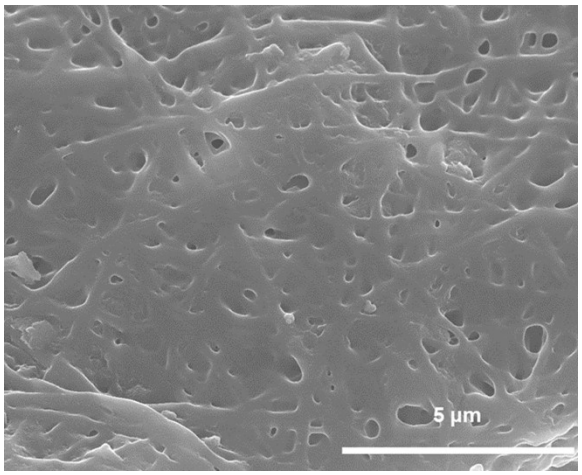

Figure S5. SEM images of PVAc after immersing in water for 30 days.

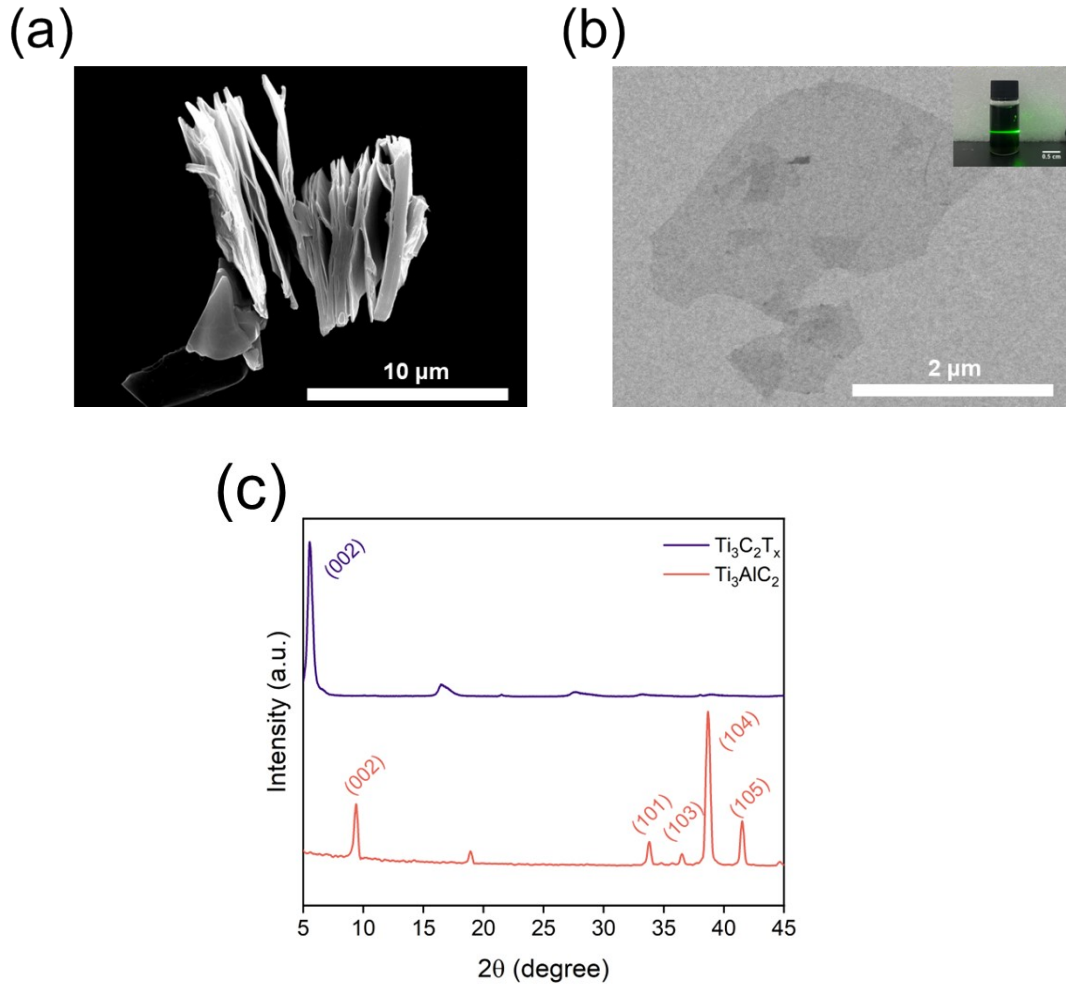

Figure S6. (a) SEM image of unpeeled multilayer MXene. (b) TEM image of single layer MXene, the inset shows the Tyndall effect of MXene suspension. (c) XRD of Ti_3AlC_2 MAX and $Ti_3C_2T_x$ MXene.

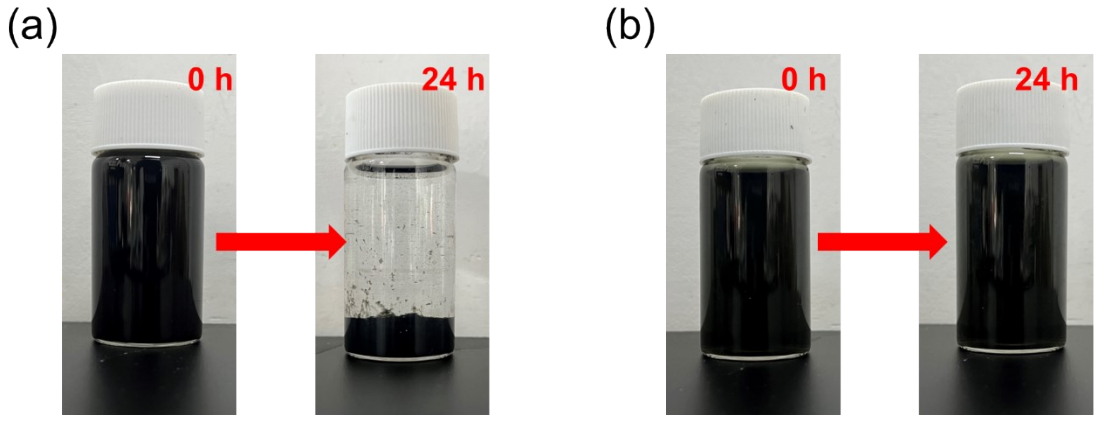

Figure S7. Digital photograph of (a) MXene/APTES suspension (the concentration of MXene is 5 mg/mL, APTES = 5 wt%) and (b) MXene suspension (the concentration of MXene is 5 mg/mL).

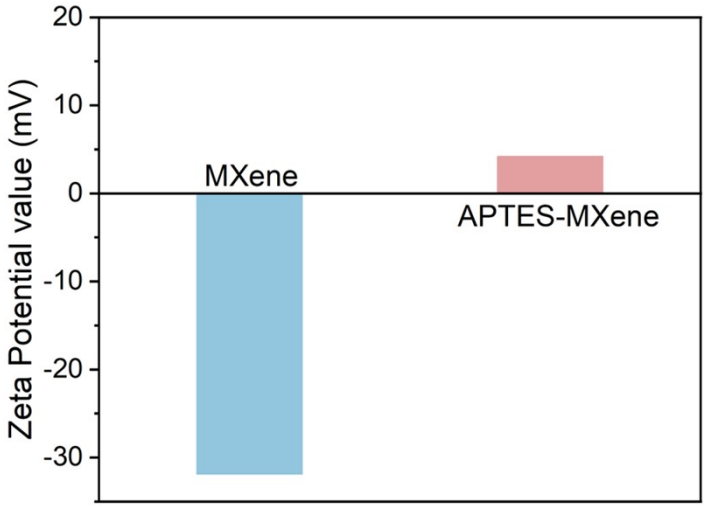

Figure S8. Zeta potential of the MXene and APTES-MXene suspensions.

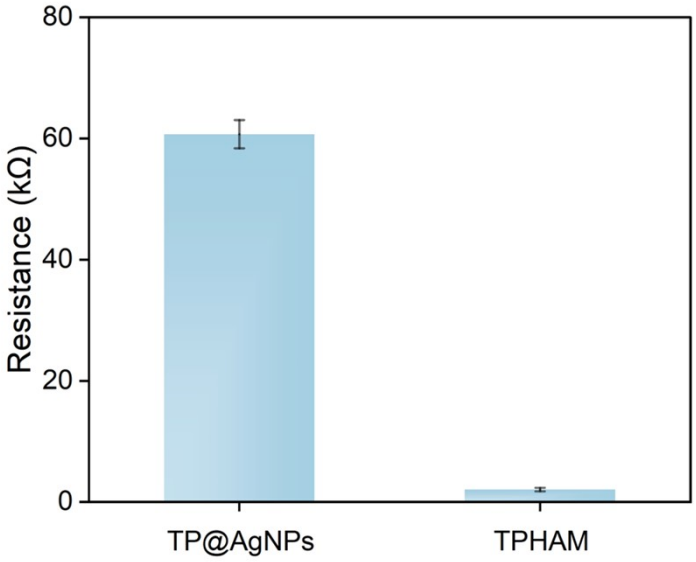

Figure S9. Resistivity comparison of TP@AgNPs and TPAMH.

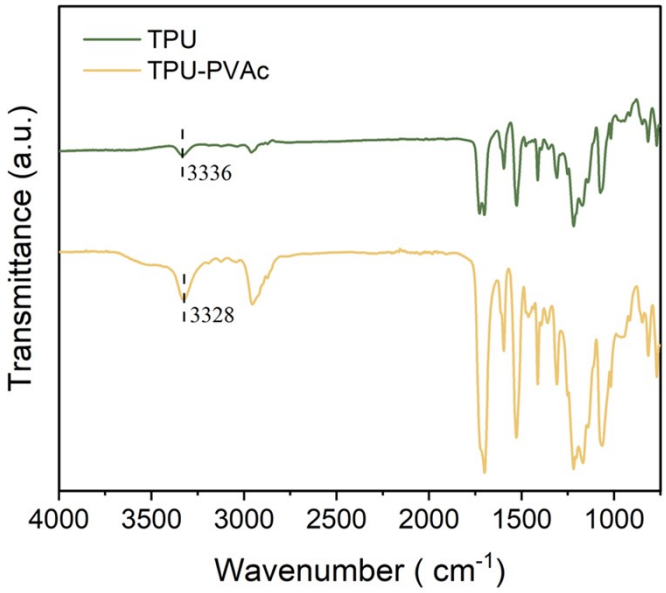

Figure S10. FTIR spectra of TPU and TPU-PVAc.

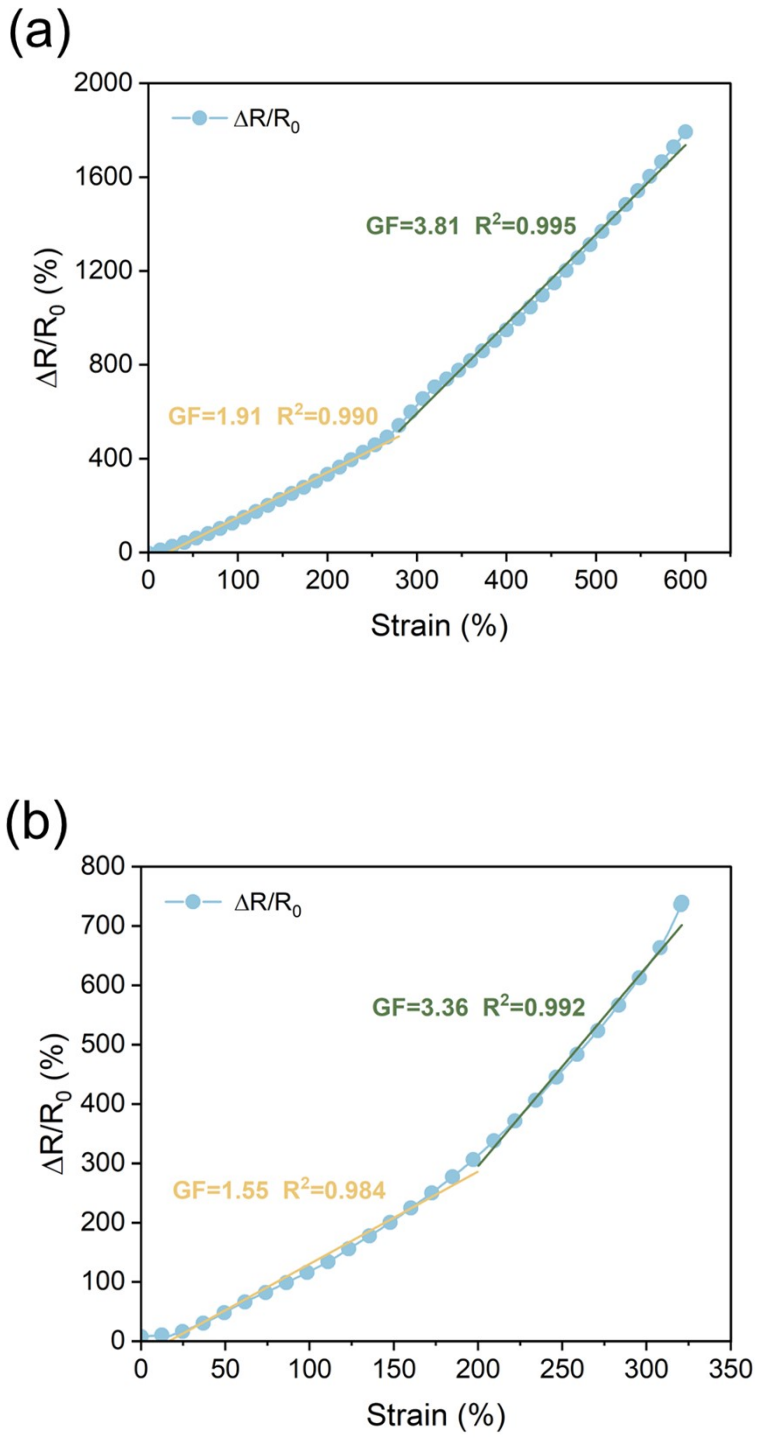

Figure S11. Relative resistance variation curves of (a)TPU-PVAc@MXene and (b) TPU-PVAc@AgNPs.

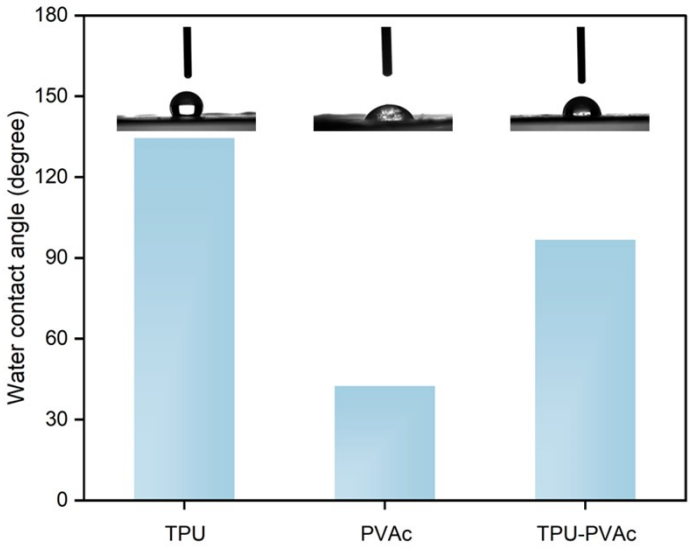

Figure S12. The water contact angle of TPU, PVAc, and TPU-PVAc.

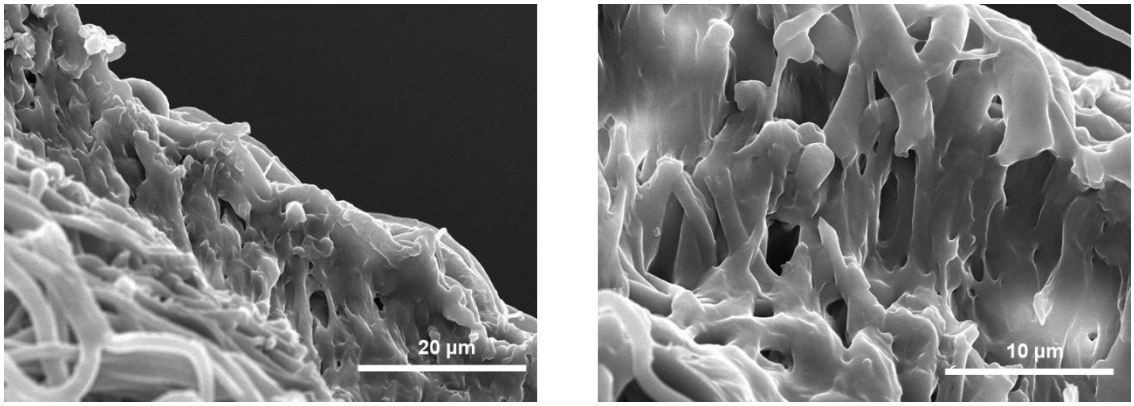

Figure S13. Cross-section SEM images of TPU-PVAc.

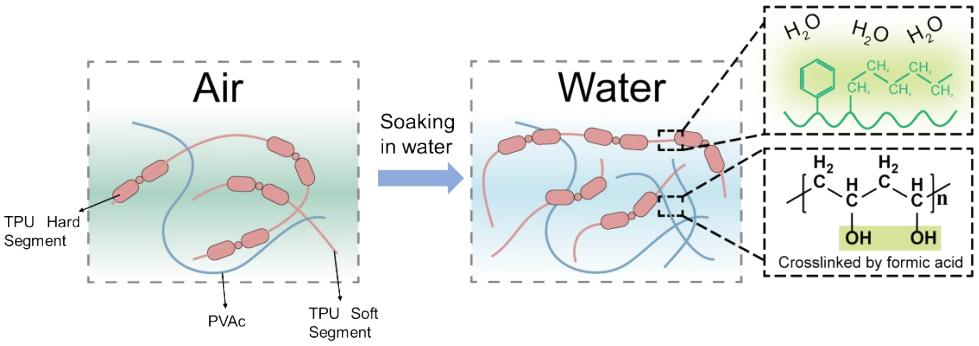

Figure S14. Scheme diagram of hydrophobic aggregation in nanofibrous hydrogel composites.

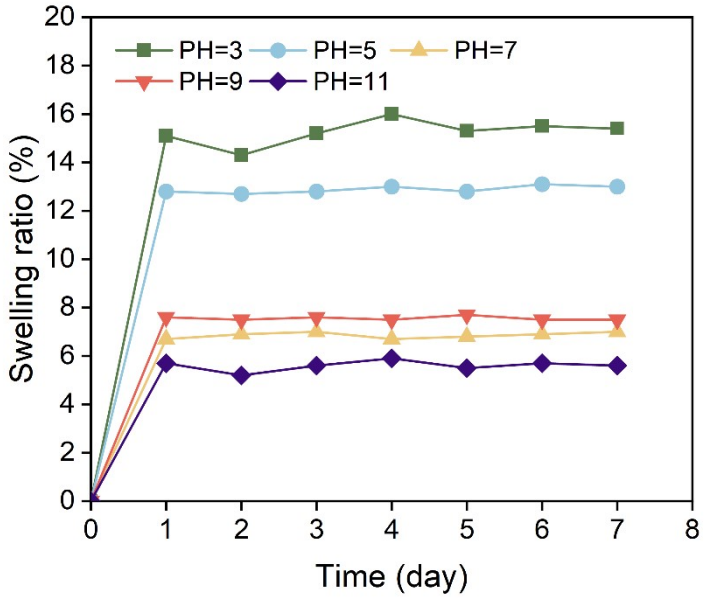

Figure S15. The swelling ratio of TPAMH in different pH environments.

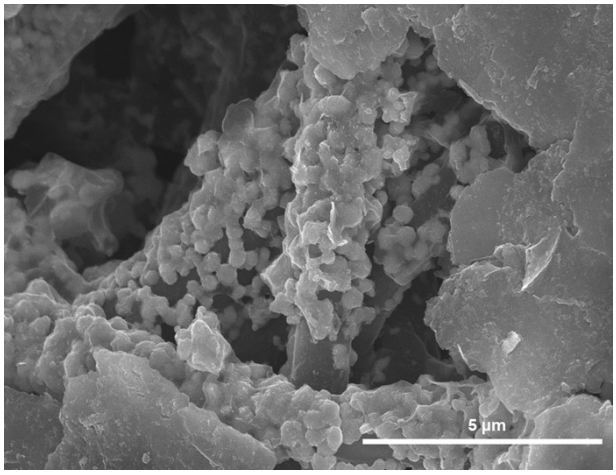

Figure S16. SEM image of TPAMH after immersing in water for 7 days.

Table S1. The swelling ratio are summarized and compared with those recent reports.

Materials	Swelling ratio	Ref.
SA(Ca^{2+})/PAA(SiO_2)	90%	Ref. [1]
PAM/cellulose	127%	Ref. [2]
PVA/P(SBMA-co-HEMA)	9%	Ref. [3]
HEAA/PEA/MEA	110%	Ref. [4]
SF/TA@PPy	11%	Ref. [5]
SA/Ca^{2+}/κ-CG/Ca^{2+}	97.39%	Ref. [6]
BA-AA-CABIL-TA	9%	Ref. [7]
P(SBMA-co-HEMA)/ cellulose	38%	Ref. [8]
PVAc nanofibrous hydrogel	5.5%	This work

Reference:

[1] W. Fan, L. R. Jensen, Y. Dong, A. J. Deloria, B. Xing, D. Yu and M. M. Smedskjaer, *ACS Appl. Bio. Mater.*, 2023, **6**, 228-237.

[2] D. Zhang, J. Jian, Y. Xie, S. Gao, Z. Ling, C. Lai, J. Wang, C. Wang, F. Chu and M.-J. Dumont, *Chem. Eng. J.*, 2022, **427**, 130921.

[3] J. Ren, Y. Liu, Z. Wang, S. Chen, Y. Ma, H. Wei and S. Lü, *Adv. Funct. Mater.*, 2022, **32**, 2107404.

[4] S. He, B. Guo, X. Sun, M. Shi, H. Zhang, F. Yao, H. Sun and J. Li, *ACS Appl. Mater. Inter.*, 2022, **14**, 45869-45879.

[5] H. Zheng, M. Chen, Y. Sun and B. Zuo, *Chem. Eng. J.*, 2022, **446**, 136931.

[6] L. Li, J. Zhao, Y. Sun, F. Yu and J. Ma, *Chem. Eng. J.*, 2019, **372**, 1091-1103.

[7] C. Sun, J. Luo, T. Jia, C. Hou, Y. Li, Q. Zhang and H. Wang, *Chem. Eng. J.*, 2022, **431**, 134012.

[8] Z. Lan, Y. Wang, K. Hu, S. Shi, Q. Meng, Q. Sun and X. Shen, *Carbohydr. Polym.*, 2023, **306**, 120541.